Reactivity oscillation in the heavy–light–heavy Cl + CH_4 reaction

Zhen Chen[a,b,1], Jun Chen[a,c,1], Rongjun Chen[a], Ting Xie[d], Xingan Wang[d], Shu Liu[a,2], Guorong Wu[a,2], Dongxu Dai[a], Xueming Yang[a,e,2], and Dong H. Zhang[a,2]

[a]State Key Laboratory of Molecular Reaction Dynamics, Dalian Institute of Chemical Physics, Chinese Academy of Sciences, 116023 Dalian, China; [b]University of Chinese Academy of Sciences, 100049 Beijing, China; [c]College of Chemistry and Chemical Engineering, Xiamen University, 361005 Xiamen, China; [d]Department of Chemical Physics, University of Science and Technology of China, 230026 Hefei, China; and [e]Department of Chemistry, School of Science, Southern University of Science and Technology, 518055 Shenzhen, China

Edited by Richard N. Zare, Stanford University, Stanford, CA, and approved March 11, 2020 (received for review October 9, 2019)

It has long been predicted that oscillatory behavior exists in reactivity as a function of collision energy for heavy–light–heavy (HLH) chemical reactions in which a light atom is transferred between two heavy atoms or groups of atoms, but direct observation of such a behavior in bimolecular reactions remains a challenge. Here we report a joint theoretical and crossed-molecular-beam study on the Cl + CH_4 → HCl + CH_3 reaction. A distinctive peak at a collision energy of 0.15 eV for the CH_3(v = 0) product was experimentally detected in the backward scattering direction. Detailed quantum-dynamics calculations on a highly accurate potential energy surface revealed that this feature originates from the reactivity oscillation in this HLH polyatomic reaction. We anticipate that such reactivity oscillations exist in many HLH reactions involving polyatomic reagents.

heavy–light–heavy | quantum differential cross-sections | reactivity oscillations | polyatomic reaction

Many important chemical reactions involve a light atom (normally a hydrogen atom) transfer between two heavy atoms or groups of atoms, which are commonly referred to as heavy–light–heavy (HLH) reactions. Because of their great practical importance and being chemically interesting, they have been the subject of numerous theoretical and experimental studies for decades (1–16). Early theoretical studies of collinear reactions on empirical potential energy surfaces (PESs) discovered pronounced but slow oscillating behavior of reaction probabilities as a function of collision energy in many HLH reactions (1–3). These oscillations were attributed to the fast chattering motion of the light atom between two heavy atoms, therefore were classical in origin (2). In late 1980, the observation of oscillatory structures in the photodetachment experiments of Neumark and coworkers on the $ClHCl^-$ and IHI^- anions greatly stimulated further theoretical studies on HLH reactions (15, 16). However, three-dimensional (3D) quantum scattering studies of triatomic reactions on increasingly realistic PESs found that the reaction probability for initial nonrotating reagent is tiny with the pronounced oscillations in the collinear reaction probability greatly suppressed (6, 9, 11). Quasiclassical trajectory simulations of HLH triatomic reactions revealed that the approach of the heavy atom tends to drive the molecule to rotate away from the collinear configuration, leading to tiny reactivity for nonrotating reagent, while initial rotation excitation can help the molecule to rotate back to collinear configuration, consequently dramatically enhancing the reactivity (11). As a result, it is hard to observe experimentally the HLH oscillation in triatomic reaction normally dominated by reagent with little rotation excitation, except by using the photodetachment technique (15, 16). An intriguing question is, can we observe such kind of oscillations in a polyatomic reaction?

The Cl + CH_4→HCl + CH_3 reaction has been the subject of extensive experimental and theoretical investigations due to its crucial role in the Cl/O_3 destruction chain mechanism in the stratosphere, and has become a prototype for studying mode specificity and bond selectivity in polyatomic reactions with a late barrier (17–36). As a hydrogen transfer reaction between the heavy Cl atom and relatively heavy CH_3 moieties, it is also an ideal HLH system for dynamics study. Earlier experimental studies found that at low collision energies the product HCl is strongly backscattered with a cold rotational state distribution (17). Crossed-molecular-beam experiments performed by Liu and coworkers on the reaction revealed that the excitation function increases steadily with collision energy with a threshold of ∼2.5 kcal/mol (21, 24). The measured angular distribution evolves slowly from backward near threshold to sideways, and into the forward hemisphere with further increase of collision energy. Banks and Clary performed a collinear quantum-dynamics study on the reaction on a high-level PES by treating the remaining spectator modes adiabatically with zero-point energy correction included (27). Their calculation not only yielded thermal rate constants in good agreement with experimental measurements, but also found oscillatory behavior in the cumulative reaction probability as observed in HLH triatomic reactions. In 2009, Czakó and Bowman constructed a high-quality global PES for the reaction system by using permutation invariant polynomial fitting (denoted as CB PES)

Significance

The hydrogen atom transfer reactions are ubiquitous in chemical and biological processes; therefore, heavy–light–heavy (HLH) reactions are of great practical importance and chemically interesting. This joint experimental and theoretical study not only shows the existence of HLH reactivity oscillation in a bimolecular reaction, but also rationalizes why such an HLH oscillation can be observed in polyatomic reactions, but not in triatomic reactions. In addition, our study represents an important progress in the dynamics study of chemical reaction with quantum differential cross-sections calculated accurately and good agreement with experiment obtained for a chemical reaction involving more than four atoms.

Author contributions: S.L., G.W., X.Y., and D.H.Z. designed research; Z.C., J.C., R.C., T.X., X.W., S.L., G.W., and D.D. performed research; Z.C., S.L., G.W., and D.H.Z. analyzed data; and S.L., G.W., X.Y., and D.H.Z. wrote the paper.

The authors declare no competing interest.

This article is a PNAS Direct Submission.

Published under the PNAS license.

[1]Z.C. and J.C. contributed equally to this work.

[2]To whom correspondence may be addressed. Email: liushu1985@dicp.ac.cn, wugr@dicp.ac.cn, xmyang@dicp.ac.cn, or zhangdh@dicp.ac.cn.

This article contains supporting information online at https://www.pnas.org/lookup/suppl/doi:10.1073/pnas.1917618117/-/DCSupplemental.

First published April 10, 2020.

Downloaded at Dalian Inst Chemical Physics on April 28, 2020

based on extensive multireference configuration interaction ab initio calculations (29, 30). On the PES, Wang and coworkers performed a six-dimensional quantum scattering study of the Cl + CH_4 reaction by treating CH_4 as a triatomic molecule (32), and Yang and coworkers carried out an eight-dimensional quantum-dynamics study of the reaction (35) by using the reduced-dimensionality model of Palma and Clary by restricting the nonreacting CH_3 group in C_{3v} symmetry (37). Both calculations revealed that there is a distinctive peak in total reaction probabilities for the total angular momentum $J = 0$ at collision energy of about 0.14 eV. Both studies inferred that the peak is related to a resonance in the reaction, however, without providing any dynamical origin. Therefore, the following questions clearly emerge: Does the oscillatory behavior observed in the collinear calculation by Bank and Clary persist in 3D calculations? What is the dynamical origin for the peak observed in these two quantum-dynamics calculations on the CB PES: dynamical resonance or HLH oscillation? How can we probe it experimentally if it does exist?

To seek answers to these questions, we present here a joint theoretical and experimental study on the reaction in the low collision energy region. The experiment was carried out on a crossed-beam apparatus in combination with time-sliced velocity map ion imaging and (2+1) resonance-enhanced multiphoton ionization (REMPI) detection of the $CH_3(v = 0)$ product (38). The experimentally measured images of the CH_3 product from the Cl + CH_4 →HCl + $CH_3(v = 0)$ reaction at collision energies of 0.12, 0.18, and 0.22 eV are depicted in Fig. 1, *Top* after the density-to-flux transformation correction. At $E_c = 0.12$ eV, the angular distribution is peaked at the backward direction (the direction of the Cl atom beam in the center-of-mass frame). With the increase of collision energy, the peak of the angular distribution moves rather quickly to sideways direction. An interesting feature for all these three images is the narrow velocity distributions close to maximum velocity limit, indicating both the CH_3 and HCl products are very cold rotationally as will be shown below. Overall, the images shown in Fig. 1 are close to those obtained by Liu and coworkers (24), except some small differences in peak positions.

It would be interesting to search if similar oscillations as those found in the reaction probability for $J = 0$ can be found in some measurable quantity such as the differential cross-sections (DCSs) at some scattering angles, as previously demonstrated in the studies of the F/Cl + HD systems (39, 40). To probe possible oscillations in reaction probabilities, we performed a careful measurement of the collision-energy dependence of DCSs in the backward scattering direction, designated as the backward scattering spectrum (BSS) for the reaction. The obtained BSS for the $CH_3(v = 0)$ product shows a clear peak at $E_c = 0.15$ eV (Fig. 2*A*). The width of the peak is about 0.08 eV (1.6 kcal/mol), larger than that observed in the F/Cl + HD reactions due to dynamical resonances.

Theoretically, we constructed an accurate full-dimensional PES for the system by using the neural-network fitting method and performed quantum-dynamics calculations by using the reduced dimensionality model of Palma and Clary with the nonreacting CH_3 group constrained in the C_{3v} symmetry (37). The calculated total reaction probabilities for the reaction on the PES for the total angular momentum $J = 0$ (Fig. 2*B*) and for J up to 100 (*SI Appendix*, Fig. S6) exhibit a clear peak structure. For $J = 0$, a distinctive peak appears at the collision energy of ∼0.14 eV, very close to that observed on the CB PES (32, 35). Because the new and CB PESs were constructed by using different fitting methods based on different level of ab initio methods, the presence of the distinctive peak on both PESs further confirmed that the peak is unlikely caused by the defects on PES. As can be seen, the peak is dominated by the $CH_3(v = 0)$ product. Interestingly, the reaction probabilities for the $CH_3(v_2 = 1)$ (v_2 is for the umbrella vibrational mode) product also exhibit a peak, but the peak energy is higher than that for $CH_3(v = 0)$ by about 0.06 eV, quite close to excitation energy of CH_3 umbrella motion of about 0.07 eV. For $J > 0$ partial waves, the peaks clearly originate from the corresponding $J = 0$ peak by progressive J shifting.

The computed 3D DCS at these three collision energies (Fig. 1, *Bottom*) for the $CH_3(v = 0)$ product reproduce well their experimental counterparts shown in Fig. 1, *Upper*. Theory also gives very cold rotational distribution for the product, with about 95% of total available energies deposited to the translational motion of the products. *SI Appendix*, Fig. S7 shows the comparison of the experimental and theoretical scattering angle distributions. The experimental DCSs involve a few low rotational states of CH_3 product covered by the bandwidth of the REMPI laser pulse, while the theoretical results include all of the rotational states of CH_3. This results in the different peak positions and relative heights in the theoretical and experimental angular distributions. We have also computed the BSS for the $CH_3(v = 0)$ product, and compared with the experimental results (Fig. 2*A*). Good agreement between theory and experiment is achieved, with the experimental BSS about 0.01 eV shifted toward higher energy. By examining the convergence of BBS with respect to partial wave function in *SI Appendix*, Fig. S8, we found that the calculated peak in BSS shown in Fig. 2*A* is contributed by partial wave function with the total angular momentum J up to 80. Despite this, the peak resembles that exhibited in the total reaction probability for the $J = 0$ partial wave in Fig. 2*B* very closely, as found in the F/Cl + HD reactions. Furthermore, the reasonable agreements between theory and experiment on DCSs and BSS indicating both the PES and quantum-dynamics method are sufficiently accurate to elucidate the dynamical origin of the observed oscillatory structure.

Does such a peak originate from an HLH oscillation or a dynamical resonance? With *S*-matrix elements for reaction available, we calculated the phases for some product states with large populations. The phases for all these states decrease steadily with collision energy, as would be expected for direct reactive scattering on a repulsive potential (*SI Appendix*, Fig. S9). The resulting lifetimes show no delay at the peak energy, indicating that the peak is not likely caused by a dynamical resonance (*SI Appendix*, Fig. S10).

To investigate the dynamical original of the reaction probability peak, we performed time-dependent wave-packet calculations to extract the scattering wave function at the collision energy of 0.14 eV (3.4 kcal/mol) for $J = 0$. The two-dimensional contour of the scattering wave function shows a distinctive peak at the corner around the saddle point without any nodal structure (Fig. 3*B*). Inspection of the wave function on the other degrees of freedom does not find any node either.

Vibrationally adiabatic potential (VAP) has been widely used to provide dynamical origin for reactive resonances in the F + H_2/HD, Cl + HD reactions (39–41). Shallow wells caused by lowered vibrational energy for the degree of freedom other than the reaction coordinate were found in VAP curves to support resonance states for these systems on highly accurate PESs. Vibrationally adiabatic treatment has also been used to study HLH reaction, because of different timescales for light atom to move across the saddle-point region and collision time which is governed by heavy-atom translational motion. On many empirical PESs for HLH systems, shallow wells were predicted in transition-state region to support dynamical resonances, in particular for that with light atom in vibrationally excited states (10, 11). Because the calculated wave function does not have any nodal structure (Fig. 3*B*), the state must

Downloaded at Dalian Inst Chemical Physics on April 28, 2020

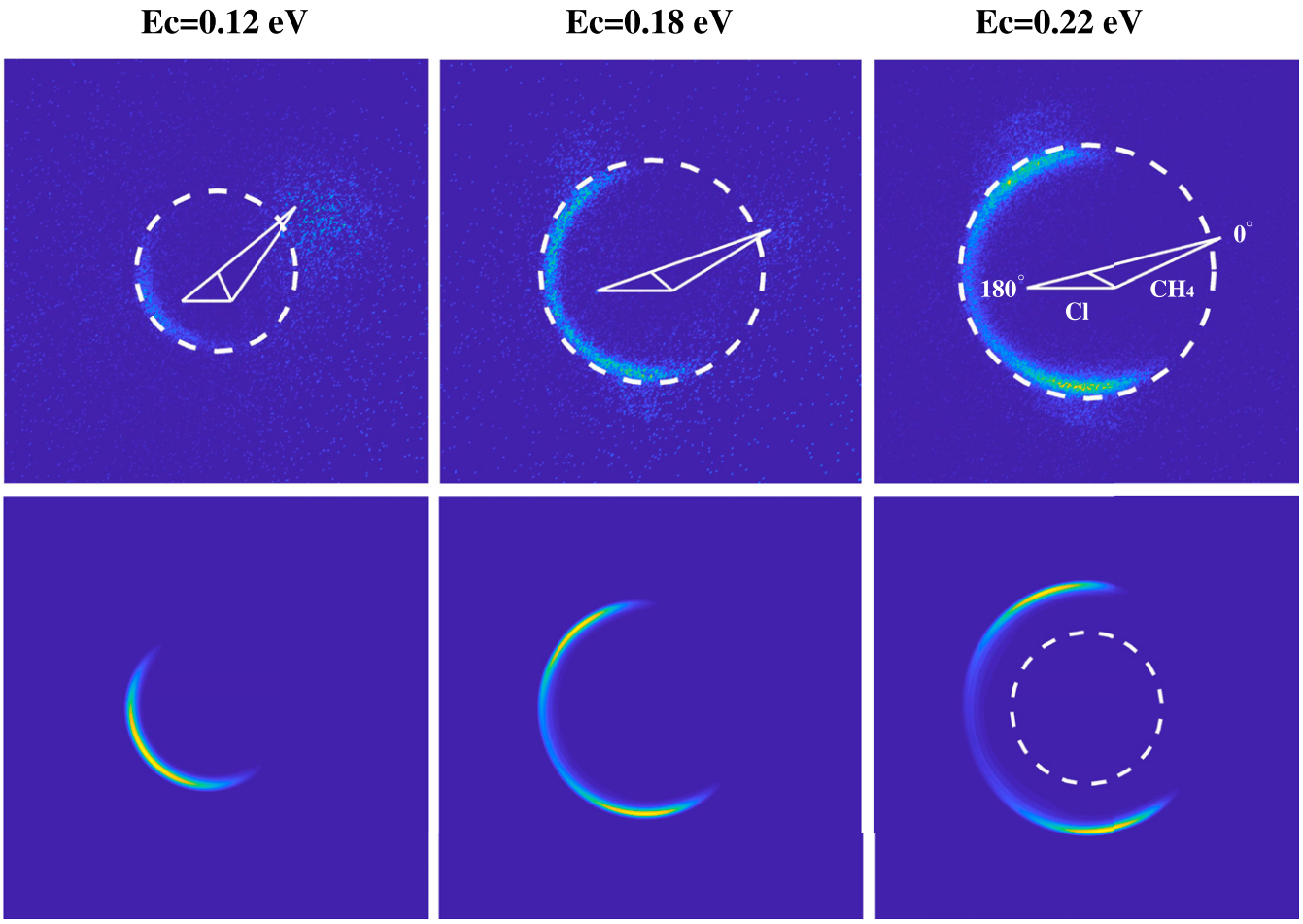

Fig. 1. (*Top*) The ion images of the $CH_3(v = 0)$ product from the Cl + CH_4 → HCl + CH_3 reaction at collision energy of 0.12 (*Left*), 0.18 (*Middle*), and 0.22 eV(*Right*). (*Bottom*) The corresponding theoretical DCSs calculated on the PES. Dashed circles represent the maximum translational energies of the product CH_3 in the ground vibrational state (*Top*) and the first umbrella excited state (*Bottom*). Newton diagrams are also shown in the figure. The experimental images involve a few low rotational states of CH_3 product covered by the bandwidth of the REMPI laser pulse, and all of the available rotational states of the coproducts, HCl. The theoretical DCSs include all of the available rotational states of CH_3 and HCl.

reside on the ground vibrational adiabatic potential surface. The calculated VAP for CH vibration in ground state does not show any well structure (*SI Appendix*, Fig. S11), confirming further the reaction probability peak is not related to a dynamical resonance. This explains why the peak energies for the $CH_3(v = 0, 1)$ product states can be different as shown in Fig. 2*B*. If these two peaks originated from a dynamical resonance, the peak positions should be the same.

To further check if the reaction probability peak is caused by HLH mass combination, we calculated the total reaction probabilities for the reaction with mass of Cl artificially reduced. With the decrease of the mass of the incoming atom, the peak becomes less prominent and disappears completely when the mass is set to 1/8 of the Cl atom (*SI Appendix*, Fig. S12). Therefore, the reaction probability peak in the reaction is the very oscillation peak for an HLH system. In other words, the HLH oscillation found by Banks and Clary in their collinear calculation persists in the reaction with nonrotating initial state (27), very different from what was observed in triatomic reactions.

From the classical point of view, the HLH oscillations originate from the fast chattering motion of the light atom between two heavy atoms/groups. To unravel how this chattering motion manifests in quantum mechanics, we present three more wave functions at the collision energies of 0.10, 0.19, and 0.24 eV (Fig. 3 *A*, *C*, and *D*), together with that of 0.14 eV. All of the wave functions have clear nodal structures in *R* direction (the distance between incoming Cl atom and CH_4 molecule) in the transition-state region which change substantially with collision energy. The nodal structures shown in Fig. 3 are standing waves in nature, originating from the superposition of the incoming wave function and reflecting wave function from the shape turning corner characteristic for an HLH system. At the collision energy of 0.10 eV (Fig. 3*A*), the first peak of the standing wave is formed largely at the reactant side of the corner due to insufficient energy. With the increase of collision energy to 0.14 eV, the first peak comes to locate exactly at the corner of the PES, leading to the peak value in reactivity. With the further increase of the collision energy, the first peak is pushed to the left side of the corner and does not have any contribution to the reaction anymore, and the second peak dominates the reaction process (Fig. 3 *C* and *D*). The reaction probability decreases from $E_c = 0.19$ eV to 0.24 eV with the second peak pushed to the left side of the corner and becoming less reactive. Therefore, the dynamical origin for the reaction probability peak in the reaction becomes clear: the relatively slow motion between Cl and CH_3 modulates the motion of transferring hydrogen atom, consequently modulating the reaction probability.

Downloaded at Dalian Inst Chemical Physics on April 28, 2020

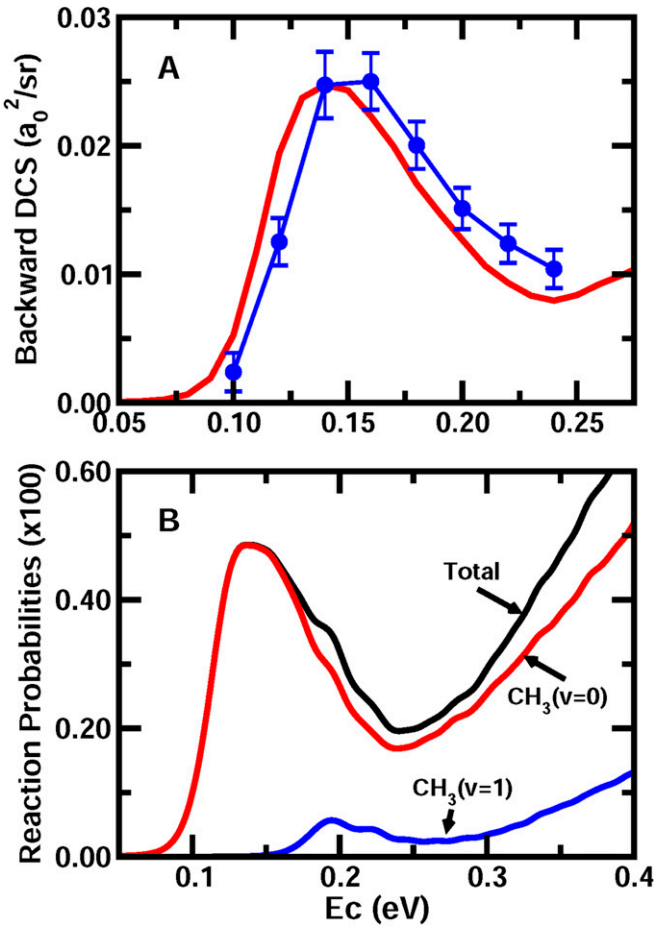

Fig. 2. DCSs in the backward-scattering direction and the $J = 0$ reaction probability as a function of collision energy. (*A*) Theoretical (solid red lines) and experimental (solid blue circles) DCS for the $CH_3(v = 0)$ product over a range of collision energies, obtained by averaging over scattering angle of 175°–185°. The experimental error bars were estimated from four independent measurements. The experimental data, measured in relative values, are scaled to the theoretical DCS value at the collision energy of 0.14 eV. (*B*) Total and product CH_3 umbrella-state-resolved reaction probabilities with $J = 0$ as a function of collision energy.

Furthermore, because the standing-wave peak shown in Fig. 3*B* is collinearly dominated, the resulting products, both HCl and CH_3, are produced rotationally cold as shown in Fig. 4 *A* and *B* for $J = 0$. With the increase of the total angular momentum, the reaction peak shifts to higher energy. As a result, the resulting cross-section also has very cold rotational distributions (Fig. 4 *C* and *D*), which is the very reason the HCl rotational distributions in ref. 17 appear that way. Why can such an oscillation be observed in this polyatomic reaction, but not in triatomic reactions? To seek the answer to this question, we carried out a series of calculation by changing the moment of inertia of the nonreacting CH_3 group (see *SI Appendix* for details). The reaction probabilities for $J = 0$ substantially decrease with the decrease of the moment of inertia (*SI Appendix*, Fig. S13). When the moment of inertia is set close to zero, equivalent to a triatomic reaction in terms of rotational motion, the reaction probabilities are much smaller than those without reduction of the moment of inertia. Therefore, it is clear that the nonreacting CH_3 group prevents in a certain extent the cleaving CH bond from rotating away quickly from the collinear configuration when the Cl atom approaches, giving more time for Cl-H-CH_3 retaining a collinear geometry in interaction region and leading

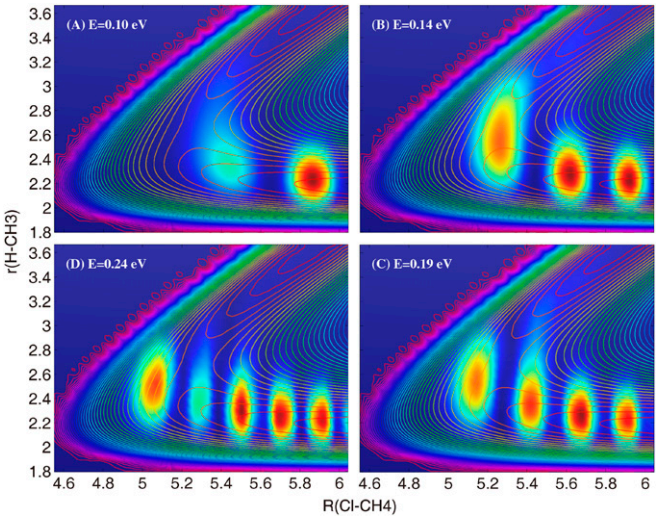

Fig. 3. Reactive scattering wave functions for the Cl + CH_4 → HCl + CH_3 reaction in the Jacobi coordinates R(Cl-CH_4) and r(H-CH_3) with other coordinates fixed at 0 at collision energies of $E_c = 0.10$ eV (*A*), 0.14 eV (*B*), 0.19 eV (*C*), and 0.24 eV (*D*).

to considerably larger reactivity than that for a triatomic HLH reaction. We also performed quasiclassical trajectory calculations at some collision energies between 0.05 and 0.5 eV (see *SI Appendix* for details). From the evolution of trajectories, we found the HLH chattering occurs at all of the energy range, which proves that the HLH chattering mechanism dominates the reaction process (*SI Appendix*, Fig. S15). We anticipate the existence of similar oscillating reactivity in many other HLH reactions involving polyatomic reagents.

Materials and Methods

The reaction was studied experimentally by using the crossed-beam apparatus in combination with time-sliced velocity map ion imaging and (2+1) REMPI techniques (38). Briefly, the Cl atom beam was generated by

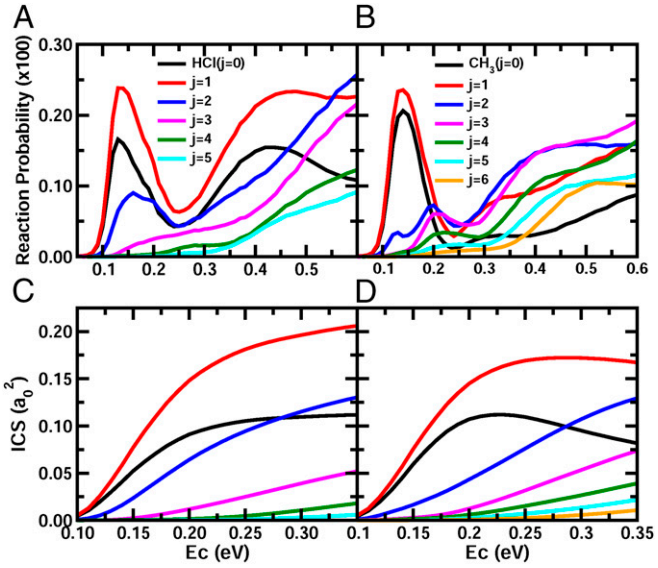

Fig. 4. Product rotational-state-resolved reaction probabilities (J = 0) and integral cross-sections for the Cl + CH_4 → HCl(j_1) + CH_3(j_2) reaction as a function of collision energy. (*A* and *B*) HCl(j_1) and CH_3(j_2) rotational-state-resolved reaction probabilities, respectively; (*C* and *D*) Same as *A* and *B* except for integral cross-sections.

Downloaded at Dalian Inst Chemical Physics on April 28, 2020

photolyzing Cl_2 (3–5% seeded in an inert carrier gas at 5 atm) with the third harmonic at 355 nm of a Nd^{3+}:yttrium aluminum garnet (Nd:YAG) laser, near the throat of a pulsed valve (General Valve). The CH_4 beam was produced from the supersonic expansion of neat CH_4 at 5 atm using an Even-Lavie valve. Both beams were collimated by a skimmer before crossing each other in a differentially pumped reaction/detection chamber. In order to vary the collision energy in a wide range, different carrier gases (He, Ne, Ar, Kr) or mixture of them for Cl_2 were used. For each carrier gas, the crossing angle between these two beams was varied to tune the collision energy in a smaller range. Images with different carrier gases for Cl_2 were scaled to each other by measuring images at one common collision energy for two neighboring collision energy ranges. The collision energy spread was estimated to be less than 10%. The CH_3 product was ionized by (2+1) REMPI method via the 3pz $^2A''$ Rydberg state (42) and recorded via the ion imaging system. The wavelength of the REMPI laser pulse (~333 nm) was fixed at the peak of the Q-branch head of the CH_3 0_0^0 band. This laser pulse (~8 mJ) was generated from a frequency-doubled dye laser output pumped by another Nd:YAG laser at 532 nm and focused by an f/160 spherical focusing lens. The polarization of laser pulse was horizontal to the plane of imaging detector. About 20,000–50,000 counting events were accumulated in each image. Background signals were also acquired and subtracted. The interaction between the CH_4 beam and the REMPI laser pulse caused a strong background in the forward direction, especially apparent at 0.12 eV (Fig. 1). Density-to-flux correction (43) was performed to all images before extracting out signal at the backward scattering direction. In such a way, the collision-energy-dependent DCS in the backward scattering direction was measured.

Theoretically, to eliminate possible defects in CB PES, we constructed a PES by using neural-network fitting based on high-level ab initio energies (*SI Appendix*). With a fitting error of ~5 meV measured in terms of root-mean-square error, the PES is expected to have a quantitative level of accuracy. More importantly, we developed a time-dependent wave-packet method to compute DCS for the reaction, and carried out extensive quantum-scattering calculations to obtain fully converged DCSs for collision energy up to 0.28 eV (*SI Appendix*). Because the CH bond length in nonreacting CH_3 group essentially does not change during the reaction, it was fixed at the equilibrium value of 1.08 Å without causing any perceptible error. Therefore, the number of degrees of freedom involved in DCS calculation is seven, representing a large quantum-dynamics calculation of DCS. With two heavy atoms (C and Cl) involved, the computation is extremely expensive, taking about 6 mo on a cluster with 36 dual-processor computers.

Data Availability. The experimental and theoretical DCS data are available in *SI Appendix*. All other data are contained in the manuscript text and *SI Appendix*.

ACKNOWLEDGMENTS. This work was supported by the National Natural Science Foundation of China (Grants 21773235, 21590804, 21688102, 21433009, and 21673234), the Chinese Academy of Sciences (Grant XDB17010200), International Partnership Program of Chinese Academy of Sciences (Grant 121421KYSB20170012), and Dalian Institute of Chemical Physics (Grant DICP ZZBS201611).

1. J. A. Kaye, A. Kuppermann, Collinear quantum mechanical probabilities for the I + HI → IH + I reaction using hyperspherical coordinates. *Chem. Phys. Lett.* **77**, 573–579 (1981).
2. E. Pollak, Classical analysis of collinear light atom transfer reactions. *J. Chem. Phys.* **78**, 1228–1236 (1983).
3. C. Hiller, J. Manz, W. H. Miller, J. Römelt, Oscillating reactivity of collinear symmetric heavy+light–heavy atom reactions. *J. Chem. Phys.* **78**, 3850–3856 (1983).
4. D. C. Clary, J. N. L. Connor, Isotope and potential energy surface effects in vibrational bonding. *J. Phys. Chem.* **88**, 2758–2764 (1984).
5. R. T. Skodje, M. J. Davis, A phase space analysis of the collinear I+HI reaction. *J. Chem. Phys.* **88**, 2429–2456 (1988).
6. G. C. Schatz, Oscillating reactivity and resonances in the three-dimensional Cl+HCl reaction. *Chem. Phys. Lett.* **151**, 409–414 (1988).
7. B. Gazdy, J. M. Bowman, A three-dimensional L^2 simulation of the photodetachment spectra of $ClHCl^-$ and IHI^-. *J. Chem. Phys.* **91**, 4615–4624 (1989).
8. G. C. Schatz, Quantum theory of photodetachment spectra of transition states. *J. Phys. Chem.* **94**, 6157–6164 (1990).
9. G. C. Schatz, D. Sokolovski, J. N. L. Connor, Resonances in heavy + light–heavy atom reactions: Influence on differential and integral cross-sections and on transition-state photodetachment spectra. *Faraday Discuss. Chem. Soc.* **91**, 17–30 (1991).
10. B. B. Grayce, R. T. Skodje, Quantum resonance dynamics for the I+HI reaction in three dimensions: An adiabatic treatment using Jacobi coordinates. *J. Chem. Phys.* **95**, 7249–7262 (1991).
11. R. T. Skodje, The adiabatic theory of heavy-light-heavy chemical reactions. *Annu. Rev. Phys. Chem.* **44**, 145–172 (1993).
12. M. Y. Hayes, M. P. Deskevich, D. J. Nesbitt, K. Takahashi, R. T. Skodje, A simple picture for the rotational enhancement of the rate for the F + HCl → HF + Cl reaction: A dynamical study using a new ab initio potential energy surface. *J. Phys. Chem. A* **110**, 436–444 (2006).
13. L. González-Sánchez *et al.*, Photodetachment spectrum of OHF^-: Three-dimensional study of the heavy-light-heavy resonances. *J. Chem. Phys.* **121**, 309–320 (2004).
14. J. Manz, K. Sato, T. Takayanagi, T. Yoshida, From photoelectron detachment spectra of $BrHBr^-$, $BrDBr^-$ and IHI^-, IDI^- to vibrational bonding of BrMuBr and IMuI. *J. Chem. Phys.* **142**, 164308 (2015).
15. A. Weaver, R. B. Metz, S. E. Bradforth, D. M. Neumark, Spectroscopy of the iodine atom + hydrogen iodide transition-state region by photodetachment of IHI. *J. Phys. Chem.* **92**, 5558–5560 (1988).
16. R. B. Metz, T. Kitsopoulos, A. Weaver, D. M. Neumark, Study of the transition state region in the Cl+HCl reaction by photoelectron spectroscopy of $ClHCl^-$. *J. Chem. Phys.* **88**, 1463–1465 (1988).
17. W. R. Simpson, T. P. Rakitzis, S. A. Kandel, T. Lev-On, R. N. Zare, Picturing the transition-state region and understanding vibrational enhancement for the Cl + CH_4 → HCl + CH_3 reaction. *J. Phys. Chem.* **100**, 7938–7947 (1996).
18. H. A. Michelsen, W. R. Simpson, Relating state-dependent cross sections to non-Arrhenius behavior for the Cl + CH_4 reaction. *J. Phys. Chem. A* **105**, 1476–1488 (2001).
19. C. Murray, B. Retail, A. J. Orr-Ewing, The dynamics of the H-atom abstraction reactions between chlorine atoms and the methyl halides. *Chem. Phys.* **301**, 239–249 (2004).
20. M. J. Bass, M. Brouard, R. Cireasa, A. P. Clark, C. Vallance, Imaging photon-initiated reactions: A study of the $Cl(^2P_{(3/2)})+CH_4 \rightarrow HCl+CH_3$ reaction. *J. Chem. Phys.* **123**, 94301 (2005).
21. B. Zhang, K. Liu, Imaging a reactive resonance in the Cl+CH_4 reaction. *J. Chem. Phys.* **122**, 101102 (2005).
22. S. Yan, Y.-T. Wu, B. Zhang, X.-F. Yue, K. Liu, Do vibrational excitations of CHD_3 preferentially promote reactivity toward the chlorine atom? *Science* **316**, 1723–1726 (2007).
23. H. Kawamata, K. Liu, Imaging the nature of the mode-specific chemistry in the reaction of Cl atom with antisymmetric stretch-excited CH_4. *J. Chem. Phys.* **133**, 124304 (2010).
24. J. Zhou, B. Zhang, J. J. Lin, K. Liu, Imaging the isotope effects in the ground state reaction of Cl+CH_4 and CD_4. *Mol. Phys.* **103**, 1757–1763 (2005).
25. B. Zhang, K. Liu, G. Czakó, J. M. Bowman, Translational energy dependence of the Cl + $CH_4(v_b = 0, 1)$ reactions: A joint crossed-beam and quasiclassical trajectory study. *Mol. Phys.* **110**, 1617–1626 (2012).
26. R. Liu *et al.*, Rotational mode specificity in the Cl + CHD_3 → HCl + CD_3 reaction. *J. Chem. Phys.* **141**, 074310 (2014).
27. S. T. Banks, D. C. Clary, Reduced dimensionality quantum dynamics of Cl + CH_4 → HCl + CH_3 on an ab initio potential. *Phys. Chem. Chem. Phys.* **9**, 933–943 (2007).
28. R. Martínez, M. González, P. Defazio, C. Petrongolo, Searching for resonances in the reaction $Cl+CH_4 \rightarrow HCl+CH_3$: Quantum versus quasiclassical dynamics and comparison with experiments. *J. Chem. Phys.* **127**, 104302 (2007).
29. G. Czakó, J. M. Bowman, Dynamics of the reaction of methane with chlorine atom on an accurate potential energy surface. *Science* **334**, 343–346 (2011).
30. G. Czakó, J. M. Bowman, Accurate ab initio potential energy surface, thermochemistry, and dynamics of the $Cl(^2P, {}^2P_{(3/2)})$ + CH_4 → HCl + CH_3 and H + CH_3Cl reactions. *J. Chem. Phys.* **136**, 044307 (2012).
31. J. R. Barker, T. L. Nguyen, J. F. Stanton, Kinetic isotope effects for Cl + CH_4 right harpoon over left harpoon HCl + CH_3 calculated using ab initio semiclassical transition state theory. *J. Phys. Chem. A* **116**, 6408–6419 (2012).
32. F. Meng, W. Yan, D. Wang, Quantum dynamics study of the Cl + CH_4 → HCl + CH_3 reaction: Reactive resonance, vibrational excitation reactivity, and rate constants. *Phys. Chem. Chem. Phys.* **14**, 13656–13662 (2012).
33. Z. Zhang, Y. Zhou, D. H. Zhang, G. Czakó, J. M. Bowman, Theoretical study of the validity of the Polanyi rules for the late-barrier Cl + CHD_3 reaction. *J. Phys. Chem. Lett.* **3**, 3416–3419 (2012).
34. Y. Li, Y. V. Suleimanov, W. H. Green, H. Guo, Quantum rate coefficients and kinetic isotope effect for the reaction Cl + CH_4 → HCl + CH_3 from ring polymer molecular dynamics. *J. Phys. Chem. A* **118**, 1989–1996 (2014).
35. N. Liu, M. Yang, An eight-dimensional quantum dynamics study of the Cl + CH_4→ HCl + CH_3 reaction. *J. Chem. Phys.* **143**, 134305 (2015).

Downloaded at Dalian Inst Chemical Physics on April 28, 2020

36. A. J. Totenhofer, J. N. Connor, G. Nyman, Angular scattering dynamics of the CH_4 + Cl → CH_3 + HCl reaction using nearside-farside, local angular momentum, and resummation theories. *J. Phys. Chem. B* **120**, 2020–2032 (2016).
37. J. Palma, D. C. Clary, A quantum model Hamiltonian to treat reactions of the type $X+YCZ_3 \rightarrow XY+CZ_3$: Application to $O(^3P)$ + CH_4 → OH + CH_3. *J. Chem. Phys.* **112**, 1859–1867 (2000).
38. G. Wu *et al*., A new crossed molecular beam apparatus using time-sliced ion velocity imaging technique. *Rev. Sci. Instrum.* **79**, 094104 (2008).
39. T. Wang *et al*., Dynamical resonances accessible only by reagent vibrational excitation in the F + HD → HF + D reaction. *Science* **342**, 1499–1502 (2013).
40. T. Yang *et al*., Reaction dynamics. Extremely short-lived reaction resonances in Cl + HD (v = 1) → DCl + H due to chemical bond softening. *Science* **347**, 60–63 (2015).
41. M. Qiu *et al*., Observation of Feshbach resonances in the F + H_2 → HF + H reaction. *Science* **311**, 1440–1443 (2006).
42. J. W. Hudgens, T. G. DiGiuseppe, M. C. Lin, Two photon resonance enhanced multiphoton ionization spectroscopy and state assignments of the methyl radical. *J. Chem. Phys.* **79**, 571–582 (1983).
43. D. M. Sonnenfroh, K. Liu, Number density-to-flux transformation revisited: Kinematic effects in the use of laser-induced fluorescence for scattering experiments. *Chem. Phys. Lett.* **176**, 183–190 (1991).

Downloaded at Dalian Inst Chemical Physics on April 28, 2020